Received: 24 February 2022 | Accepted: 28 March 2022

DOI: 10.1002/sia.7095

RESEARCH ARTICLE

SURFACE and INTERFACE ANALYSIS WILEY

QUEELS: Software to calculate the energy loss processes in TEELS, REELS, XPS and AES including effects of the core hole

Sven Tougaard[1] | Nicolas Pauly[2] | Francisco Yubero[3]

[1]Department of Physics, Chemistry and Pharmacy, University of Southern Denmark, Odense M, Denmark

[2]Université libre de Bruxelles, Service de Métrologie Nucléaire (CP 165/84), Brussels, Belgium

[3]Instituto de Ciencia de Materiales de Sevilla, Univ. Sevilla - CSIC, Sevilla, Spain

Correspondence
Sven Tougaard, Department of Physics, Chemistry and Pharmacy, University of Southern Denmark, DK-5230 Odense M, Denmark.
Email: svt@sdu.dk

We present the user-friendly and freely available software package QUEELS (QUantitative analysis of Electron Energy Losses at Surfaces) that allows to calculate effective inelastic scattering cross sections within the dielectric response description, for swift electrons travelling nearby surfaces in several environments. We briefly describe the underlying theoretical models and illustrate its use to evaluate the distribution of energy losses taking place in electron spectroscopies like transmission electron energy loss spectroscopy (TEELS), X-ray photoelectron spectroscopy (XPS), Auger electron spectroscopy (AES) and reflection electron energy loss spectroscopy (REELS), which are widely used for material analysis. This includes the intrinsic excitations due to the core hole in XPS and AES.

KEYWORDS
AES, electron energy loss, QUEELS software, REELS, surface effects, TEELS, XPS

1 | INTRODUCTION

The importance of electron spectroscopies for surface analysis is widely recognized, and X-ray photoelectron spectroscopy (XPS), Auger electron spectroscopy (AES), transmission electron energy loss spectroscopy (TEELS) and reflection electron energy loss spectroscopy (REELS) provide detailed information on the elemental composition, the chemical properties and the electronic structure of surfaces.[1] A common feature among these techniques is electron transport within the surface region of the materials that will change the energy distribution of the originally excited electrons. This is due to the inelastic scattering events experienced by the electrons as they travel in matter and vacuum on their way to the detector. Consequently, quantitative interpretation of spectra from these techniques requires a good understanding of the inelastic scattering processes undergone by electrons travelling within the surface region of the studied material. For XPS and AES, there are additional so-called intrinsic excitations caused by the sudden creation of a static core hole.

Dielectric response theory has been extensively used to describe transport-induced electron energy losses. In 1954, Lindhard[2] developed a model for electrons moving in a homogeneous isotropic medium, which sets the basic relationship between the dielectric properties of the material and the corresponding distribution of the electron energy losses. A few years later, Ritchie[3] determined the energy distribution of fast electrons passing through a thin foil using the linearized hydrodynamical equations of Bloch. This was the first theoretical demonstration of surface plasmon excitations. The same approach was considered by Yubero and Tougaard in 1992[4] to account for the energy losses of electrons travelling in a reflection trajectory normal to a surface. A few years later, within the so-called surface reflection model proposed by Ritchie and Marusak[5] and Gervasoni and Arista,[6] this model was further expanded to handle 'V-type' reflection trajectories with any incident and exit angles[7] to account for the electron energy losses measured in typical REELS experiments. Then, in 1997, Simonsen et al.,[8] using the same surface reflection model, calculated the energy losses by emitted electrons in the presence of a static positive charge, which corresponds to the

case of photoelectron/Auger emissions in XPS/AES experiments. The theoretical expressions, in particular for the REELS and XPS/AES situations, are very complex. This is a major hindrance for general practical application of these models, and the main motivation for developing the present software is to make these model calculations easily available for general use.

It is worth mentioning that alternative models have been proposed by other authors to account for electron energy losses in either REELS or XPS experiments. They mostly consider separate and independent expressions for bulk and surface energy losses with specific dielectric function dependence, and the total energy loss is obtained by a linear combination of these.[9] This approximation is based on the saturation expression of the surface plasmon probability obtained by Ritchie[3] for electron energy losses, valid for transmission through thin foils with large thickness where interferences between the surface modes excited at the two foil surfaces vanishes.[10] It is however important to note that the energy loss processes cannot in general be described as a simple linear combination of a bulk and a surface contribution to the energy loss because they interfere in a complex way.[4,11] This effect can also easily be demonstrated and evaluated with the present QUEELS software.

Other groups have derived position-dependent inelastic scattering cross sections for REELS. In particular, theoretical derivation of the 'differential inverse inelastic mean free path' (which we, for convenience, denote 'cross section' in this and in our previous papers) for electrons moving close to a surface were performed by Li et al.[12] considering a dielectric response theory and by Ding[13] using a quantum mechanical self-energy formalism.

In QUEELS, the electron energy losses are evaluated within the dielectric response approximation assuming the electrons follow straight-line trajectories and thus neglecting the effect of small angle elastic deflections. The only effect ascribed to elastic scattering is for the backscattering event in reflection electron trajectories. In this latter case, electron trajectories are considered as V-type; that is, the electron is reflected in a single large angle scattering event (see Figure 1C). This was shown by extensive Monte Carle simulations to be a reasonable approximation.[14] Within this model, analytical expressions for the energy losses were obtained and the resulting analytical expressions for the inelastic scattering cross sections obtained for the different situations depend in a complex way on the geometry and the dielectric function.

To make numerical evaluation of these distributions of electron energy losses easily available to the general user, Tougaard and Yubero developed a user-friendly software QUEELS (QUantitative analysis of Electron Energy Losses at Surfaces).[15,16] It allows to calculate energy losses of electrons travelling nearby surfaces in configurations that correspond to the individual electron trajectories found in TEELS, REELS, XPS and AES experiments (see Figure 1). The software calculates an effective cross section K_{eff}, which is the *average* probability that the electron shall lose a certain energy per unit energy loss and per unit path length travelled *inside* the solid. It is noted that the electron will also undergo energy loss processes as it moves in the vacuum above the surface. This is due to the interaction of the electron of charge −e, with its positive image charge which it induces in the material. When the electron travels away from the surface, it will be decelerated by the force from the positive image charge, which adds a positive contribution to the cross section. For the REELS situation (Figure 1C), the electron is, on its way to the surface, accelerated by the positive image charge, which corresponds to a negative contribution to the cross section. These contributions are included in the total energy loss. But note that the average is calculated per unit path length the electron has travelled *inside* the solid.

As an example, Figure 2 shows the effective inelastic scattering cross sections calculated for an electron of 2000 eV kinetic energy travelling the same pathlength of 20 Å in gold, considering the following situations: (A) a homogeneous isotropic medium, (B) passing through a 20 Å thin foil at normal incidence, (C) being backreflected at a depth 10 Å below the surface (with normal incidence and reflection paths) and (D) emitted in a situation where a static positive charge q = +e is created at the same time as the electron in a trajectory normal to the surface. With q = +e, this corresponds to photon excited electron emission while q = +2e corresponds to Auger electron emission. Differences between the energy loss distributions in these configurations are noticeable due to the specific interaction of the swift electron with surfaces and/or static positive charge along their paths.

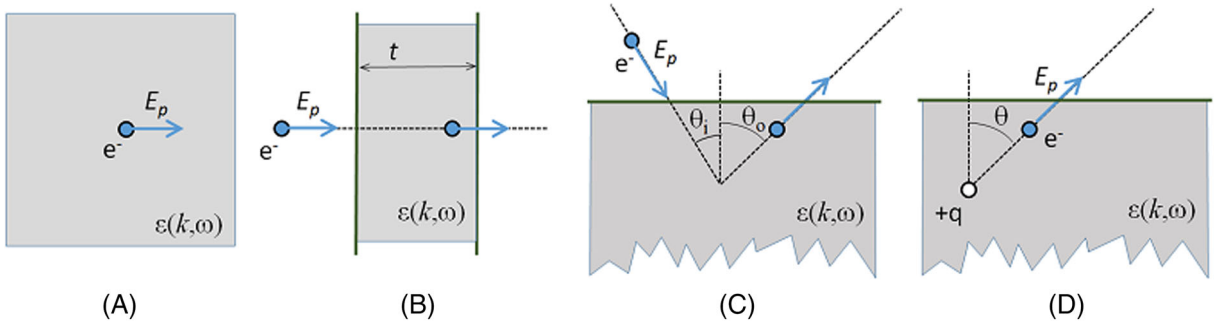

FIGURE 1 Schematic representation of the environments in which QUEELS allows to evaluate energy losses of swift electrons with primary kinetic energy E_p travelling in matter characterized by its dielectric function $\varepsilon(k,\omega)$: (A) homogeneous isotropic medium, (B) through a thin foil, (C) V-type reflection at a surface and (D) emitted in presence of a static positive charge corresponding to photoelectron or Auger electron emission

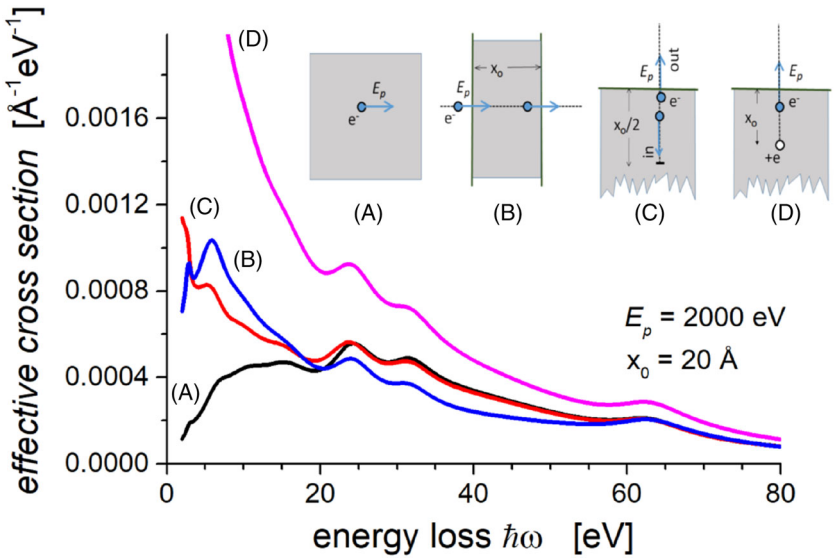

FIGURE 2 Effective inelastic scattering cross sections for electrons with 2000 eV kinetic energy that have travelled a distance $x_0 = 20$ Å in gold in (A) a homogeneous isotropic medium, (B) through a thin foil, (C) in a backreflected trajectory and (D) emitted normal to the surface in the presence of a static positive charge +e

Compared with the electron travelling in the interior of gold (A), the electrons in the other situations have a larger effective cross section due to the extra contribution from excitations when the electron is in the near surface region and in the vacuum, while the electron in (D) corresponding to photo emission has an additional significant increase of energy loss due to the excitations set up by the suddenly created core hole ('intrinsic' excitations) and to the attraction of the moving electron by the static positive core hole. The software allows to calculate the separate contributions to the energy loss from the path travelled in vacuum (both towards and away from the surface) and also for the path travelled inside the material.[4,7] It is instructive to explore, for example, how these individual contributions in the vacuum can be negative for the path to the surface (in the REELS geometry, Figure 1C), corresponding to a gain in energy from the attraction by the positive image charge.

In the present paper, we describe the practical use of the software, which is now freely available.[15] It is noted that the QUEELS software calculates the contribution from individual electrons in the various geometries and is well suited to explore the general interactions. For TEELS, this corresponds directly to the experimental situation while for REELS and XPS/AES, the experimental spectrum will typically have contributions from a range of electron trajectories. To make a direct quantitative comparison to experiment in these cases, one must make an average over the energy loss for the corresponding range of electron trajectories. This is done in the softwares QUEELS-$\epsilon(k,\omega)$-REELS and QUEELS-XPS software packages.[17,18]

In the past 25 years, the theory implemented in the QUEELS software has been applied to explore the influence of energy loss in these situations.[7,8,11,14,16,19–21] The quantitative agreement with experiment for both REELS,[22,23] XPS[16] and AES[24,25] as well as the consistent agreement when the experimental geometry is varied have been found to be good. Furthermore, calculated XPS spectra were found in references[26,27] to be in good quantitative agreement with first principle quantum mechanical calculations of the detailed excitations in primary excitation spectra for CuO and Fe_2O_3, respectively. These results give confidence in the validity as well as the accuracy of the models behind, also for the individual electron trajectories handled in the present QUEELS software.

The paper is structured to guide interested scientists in the use of the QUEELS software. The general theory behind the dielectric response description of electron energy losses implemented in the software is summarized in Section 2. Sections 3 to 6 illustrate, with some case examples, the possibilities of the software to evaluate energy distributions for electrons travelling in different environments: homogeneous isotropic medium (Section 3), through a thin foil (Section 4), backreflected from a surface (Section 5) and emitted in the presence of a static positive charge (Section 6). Finally, Section 7 gives a short user's guide to the software. An extended version of the user's manual is given in the supporting information.

2 | GENERAL THEORETICAL BACKGROUND

2.1 | Inelastic scattering cross section

The dielectric response theory allows to calculate the effective inelastic scattering cross section $K_{eff}^{env}(\hbar\omega)$ where $K_{eff}^{env}(\hbar\omega)\cdot d\hbar\omega$ is the probability for an electron travelling with kinetic energy E_p in a material characterized by its dielectric function $\varepsilon(k,\omega)$ to lose energy in the interval $\hbar\omega,d\hbar\omega$ per unit path length travelled *inside* the medium. The superscript *env* refers to the four different environments that can be evaluated with the QUEELS software (see Figure 1). In the theoretical models, it is assumed that the electron kinetic energies are non-relativistic and much larger than the energy losses considered (i.e., $\hbar\omega << E_p$). The inelastic scattering cross section takes the general form[8]:

$$K_{eff}^{env}(\hbar\omega) = \frac{-1}{8\pi^4 x_0 \hbar^2 \omega \int dt \int d\boldsymbol{r}} \rho_{ext}(\boldsymbol{r},t)\, Re\left\{ i \int d\boldsymbol{k}\, \boldsymbol{kv}\, \Phi_{ind}(\boldsymbol{k},\omega) e^{i(\boldsymbol{kr}+\omega t)} \right\} \tag{1}$$

where $\rho_{ext}(\boldsymbol{r},t)$ is the charge density of the swift electron, $\boldsymbol{v}$ the primary electron velocity ($v^2 = 2E_p/m$, with m the electron mass) and t, $\boldsymbol{r}$ and $\boldsymbol{k}$ are time, space and momentum variables. $\Phi_{ind}(\boldsymbol{k},\omega)$ is the induced potential set-up by the external charges considered (i.e., the swift electron and for XPS and AES an additional static positive charge). Equation 1 is obtained by comparing two expressions for the stopping power $S(E_p)$: either calculated from the cross section

$$S(E_p) = \int_0^\infty d\hbar\omega\, \hbar\omega K_{eff}^{env}(\hbar\omega) \tag{2}$$

or expressed as the energy loss from the force exerted on the moving electron by the induced potential $\Phi_{ind}(\boldsymbol{r},t)$

$$S(E_p) = -\frac{1}{x_0} \int d\boldsymbol{r} \int dt\, \rho_{ext}(\boldsymbol{r},t) \vec{v} \cdot \overrightarrow{\nabla \Phi_{ind}}(\boldsymbol{r},t) \tag{3}$$

where x_0 is the path travelled *inside* the material. The induced potential is found by solving the Poisson equation in Fourier space considering the appropriate external charge distribution

$$\varepsilon(k,\omega)\Phi_{ind}(k,\omega) = \left(4\pi/k^2\right)\left[\rho_{ext}(k,\omega) + \sigma(k,\omega)\right] \tag{4}$$

where $\sigma(k,\omega)$ takes different values depending on the boundary conditions of the particular system.[7,8]

It is convenient to express the obtained effective inelastic scattering cross sections $K_{eff}^{env}(\hbar\omega)$ as the sum of the contributions due to the interaction of the moving electron in a homogeneous isotropic material $K(\hbar\omega)$ plus correcting terms $K_{eff}^{env-corr}(\hbar\omega)$ due to the specific interaction with surfaces and/or a static positive charge:

$$K_{eff}^{env}(\hbar\omega) = K(\hbar\omega) + K_{eff}^{env-corr}(\hbar\omega) \tag{5}$$

Note that $K_{eff}^{env-corr}(\hbar\omega)$ cannot be calculated directly but is found by subtracting $K(\hbar\omega)$ (Equation 12) from the determined $K_{eff}^{env}(\hbar\omega)$.

The QUEELS software also allows to determine effective inelastic mean free paths $\lambda_{eff}(E_p)$ for the electron in the different environments. It is noted that, traditionally, the well-known electron inelastic mean free path (IMFP) $\lambda(E_p)$ refers to the assumption that the electron is moving in a homogeneous isotropic material.[28] This corresponds to case (A) in Figures 1 and 2. However, for practical situations corresponding to situations (B), (C) and (D), the energy loss is larger (see Figure 2) and consequently the effective inelastic mean free path $\lambda_{eff}(E_p)$ defined as the inverse of the integral of the cross section will be smaller

$$\lambda_{eff}(E_p) = \left[\int_0^\infty d\hbar\omega\, K_{eff}^{env}(\hbar\omega)\right]^{-1} \tag{6}$$

In practice, $K_{eff}^{env}(\hbar\omega)$ is only evaluated to an upper limit E_{max} (typically about 100 eV) because the dielectric function is often not available for larger energies. So, to also account for the contribution from deeper core levels, the effective inelastic mean free path is obtained as

$$[\lambda_{eff}(E_p)]^{-1} = \int_0^{E_{max}} d\hbar\omega\, K_{eff}^{env}(\hbar\omega) + [\lambda_c(E_p)]^{-1} \tag{7}$$

where $\lambda_c(E_p)$ is a correction term that accounts for energy losses due to the interaction with deep core levels. Powell[29] found that this latter contribution can be estimated by the expression

$$\lambda_c(E_p) = \frac{E_p}{a_c(\ln E_p + b_c)} \tag{8}$$

where a_c and b_c are tabulated in reference.[30]

2.2 | Dielectric response of the medium

The imaginary part of the inverse of the dielectric function, $Im\{-1/\varepsilon(k,\hbar\omega)\}$, denoted the energy loss function (ELF), is the leading function that describes the material response to account for energy losses of swift electrons in matter. For this reason, it is a practical advantage to express the dielectric function in the form of a parametrized ELF, instead of the dielectric function itself, as input for the calculation of inelastic scattering cross sections. In QUEELS, the dielectric response of the material is expressed as a sum of Drude–Lindhard-type oscillators as[7,31]

$$Im\left\{-\frac{1}{\varepsilon(k,\hbar\omega)}\right\} = \theta(\hbar\omega - E_g) \cdot \sum_{i=1}^{n} \frac{A_i\, \hbar\gamma_i\, \hbar\omega}{\left[(\hbar\omega_{0ik})^2 - (\hbar\omega)^2\right]^2 + (\hbar\gamma_i)^2 (\hbar\omega)^2} \tag{9}$$

with the momentum dispersion relation

$$\hbar\omega_{0ik} = \hbar\omega_{0i} + \alpha_i \frac{\hbar^2 k^2}{2m} \tag{10}$$

where A_i, $\hbar\omega_{oi}$, $\hbar\gamma_i$ and α_i denote the strength, position, width and dispersion parameters of the ith ELF oscillator. The step function $\theta(\hbar\omega - E_g)$ (= 1 for $\hbar\omega > E_g$ and 0 for $\hbar\omega < E_g$) is included to describe the fact that the electron cannot lose energy less than the band gap energy E_g in semiconductors and insulators while $E_g = 0$ for metals.

To ensure that the parametrized ELF fulfils the Kramers–Kronig relations in the optical limit, the oscillator strengths A_i in Equation 9 must be chosen to fulfil the optical sum rule.[32]

$$\frac{2}{\pi}\int_0^\infty \frac{d\hbar\omega}{\hbar\omega} Im\left\{\frac{1}{\varepsilon(\hbar\omega)}\right\} = 1 - Re\left\{\frac{1}{\varepsilon(0)}\right\} \quad (11)$$

In Equation 11, $Re\{1/\varepsilon(0)\}$ is the real part of the inverse of the dielectric function in the optical limit (note that for metals $Re\{1/\varepsilon(0)\} << 1$ and for insulators $Re\{1/\varepsilon(0)\} \cong 1/n^2$, where n is the refractive index in the visible range of the electromagnetic spectrum).

During the past years, several authors have determined parametrized ELF for many materials and to facilitate the practical use of the software, a database with ELF dielectric functions for various materials is available.[33]

3 | ELECTRONS MOVING IN A HOMOGENEOUS ISOTROPIC MEDIUM

The inelastic scattering cross section $K(\hbar\omega)$ for a swift electron travelling in a homogeneous isotropic medium is given by the well-known expression from Lindhard[2]:

$$K(\hbar\omega) = \frac{1}{\pi E_p a_0}\int_{k_-}^{k_+} dk \frac{1}{k} Im\left\{-\frac{1}{\varepsilon(k,\hbar\omega)}\right\} \quad (12)$$

Here, $a_0 = 0.53$ Å is the Bohr radius and the integration limits correspond to the minimum and maximum possible momentum transfer by the swift electron to the medium $k_\pm = \sqrt{2m/\hbar^2}\left[\sqrt{E_p} \pm \sqrt{E_p - \hbar\omega}\right]$.

Figure 3 shows, as an example, the cross section in gold for electrons with 500, 1000 and 2000 eV kinetic energy, respectively. Note that the shape of the curves is similar while the absolute value decreases with increasing energy, which, by Equation 6, corresponds to an increasing IMFP.

Applications of K are extremely large. For a given ELF, it can be used to calculate the IMFP as a function of energy. K and the IMFP can also be used as input data for Monte Carlo simulations[34] and as input for accurate determination of the structure and composition of nano-structures with the QUASES software package (Quantitative Analysis of Surfaces by Electron Spectroscopy).[35] In QUASES, the two- or three-parameter universal inelastic scattering cross section developed by Tougaard[36] is generally used with good results; however, in some cases, it can be an advantage to use the specific cross section of a given material.

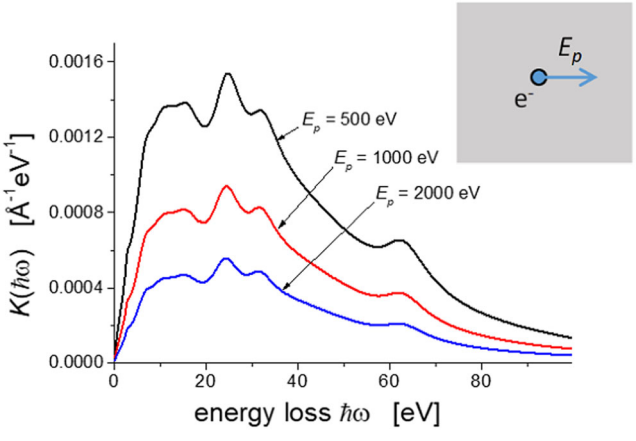

FIGURE 3 Inelastic scattering cross section K corresponding to electrons travelling in gold with 500, 1000 or 2000 eV kinetic energy

4 | ELECTRONS PASSING THROUGH A THIN FOIL (TEELS)

An analytical expression for the probability for energy losses of electrons passing normal to the surface through a thin foil was first obtained by Ritchie.[3] He found that, for a thin foil of thickness t, the corresponding inelastic scattering cross section $K_{eff}^{tf}(\hbar\omega)$ can be written as[3]

$$K_{eff}^{tf}(\hbar\omega) = K(\hbar\omega) + K_{eff}^{tf-corr}(\hbar\omega) \quad (13)$$

where the first term $K(\hbar\omega)$ corresponds to energy losses in a homogeneous isotropic medium (Equation 12) and the second term $K_{eff}^{tf-corr}(\hbar\omega)$ corresponds to the corrections due to the interaction of the swift electron with the fields set up at the foil boundaries. In the limit of large foil thicknesses in which case the fields set up at the two foil surfaces do not interfere, the correction term $K_{eff}^{tf-corr}(\hbar\omega)$ can be written as a sum of two contributions whose material dependence are roughly of the form $-Im\{1/\varepsilon\}$ and $Im\{1/(\varepsilon+1)\}$, which correspond to a diminished probability for bulk excitations (the so-called Begrenzung effect) and to an increase in surface plasmon excitations, respectively. Note however that for small foil thickness where surface excitations in both sides of the foil interfere, $K_{eff}^{tf-corr}(\hbar\omega)$ depends on the dielectric function in a rather involved way.[3]

Figure 4A,B shows the inelastic scattering cross sections for electrons travelling through gold foils of various thicknesses and the corresponding surface correction obtained for primary electrons of 100 keV. Note that the surface contribution is enhanced at small energy losses and its relative contribution to the total cross section decreases for increasing foil thicknesses.

Such calculations may be used to determine the ELF of a foil material by a trial-and-error procedure varying the oscillator parameters (in Equation 9), which describe the ELF, until a good match is achieved between experimental TEELS spectra of an unknown sample (after correction for multiple inelastic scattering) and simulated $K_{eff}^{tf}(\hbar\omega)$ obtained with QUEELS.

As an example, Figure 5 shows a comparison between single collision spectra obtained in a TEELS experiment[37] with 100 keV electrons on a 406 Å thick ZnO foil. The ratio of thickness to inelastic mean free path is 0.42 (considering the inelastic mean free path of 969 Å calculated with free QUASES-IMFP-TPP2 software[38] that allows to take relativistic effects into account). For this example, we have not attempted to determine the ELF, but we just used the ELF determined earlier[39] from analysis of experimental REELS spectra through analysis with *QUEELS-ε(k,ω)REELS software*[17]

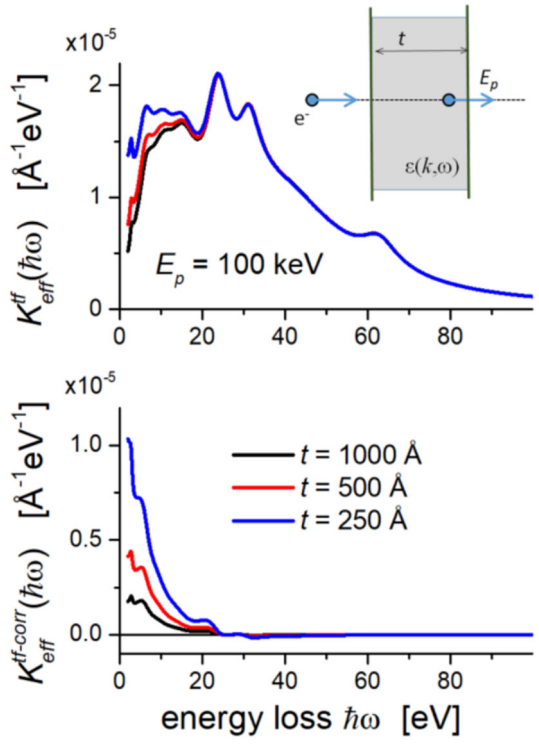

FIGURE 4 Effective inelastic scattering cross section $K^{tf}_{eff}(\hbar\omega)$ (top) and corresponding surface correction contribution $K^{tf-corr}_{eff}(\hbar\omega)$ (bottom) for swift electrons of 100 keV passing through gold foils of various thicknesses

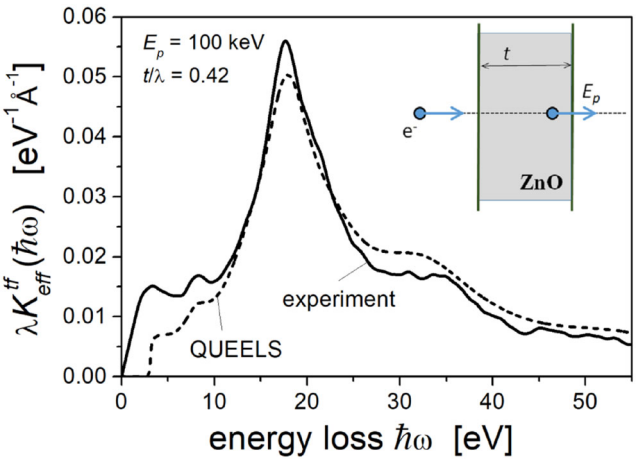

FIGURE 5 Normalized energy-differential inelastic scattering cross sections $\lambda K^{tf}_{eff}(\hbar\omega)$ obtained for 100 keV electrons crossing a ZnO foil with ratio of thickness to inelastic mean free path t/λ of 0.42. Experimental results[37] (solid line) and QUEELS simulations (dashed line) are shown

(this provides general facilities to determine the ELF from analysis of REELS), and despite of this, the agreement is seen to be very good.

5 | ELECTRONS REFLECTED AT A SURFACE (REELS)

Analytical expressions to evaluate the probability for energy losses of swift electrons reflected at the surface of a material, characterized by its dielectric function, were found by Yubero et al.[4,7] In the following subsections, we describe the basic theory and the procedure to evaluate this with QUEELS.

5.1 | Normal incidence and exit angles

First, consider a swift electron with primary kinetic energy E_p that travels from vacuum towards a semi-infinite medium (characterized by its dielectric function) at normal incidence, and after crossing the surface and penetrating to a depth x_0 inside the material, the electron is backreflected through the same path (i.e., backscattered in a single elastic event by 180°). This situation was studied in reference,[4] where the goal was to determine to what extent, for a typical electron trajectory in a REELS experiment, the field set-up in the medium by the electron in the incoming path of its trajectory dies out or is still present when the backscattered electron passes the same region on its way out. This was done by considering two extreme cases: Model A, in which the electron energy losses in the incoming and outgoing electron trajectories are evaluated independently (i.e., without including the interference between the field set-up by the electrons in the incoming and outgoing trajectories), or Model B, where the field set-up in the incoming path of the electron trajectory interacts with the swift electron on its way out after being backscattered. Figure 6 shows a schematic representation of these two extreme situations.

A complete study of this interference effect was performed in reference.[4] It was found that the corresponding effective inelastic mean free path varies not only with electron energy but also with the depth at which the elastic scattering event takes place.[4] Figure 6 shows as an example, the comparison of inelastic scattering probability distributions calculated with QUEELS for electrons backscattered in gold at 10 Å depth with several primary kinetic energies obtained from Model A and Model B, respectively. There is a clear effect of the field set up by the incoming electron and it must therefore be included in the model.

5.2 | Any incidence and exit angles within a V-type reflection trajectory

Having found that there is a strong difference between Models A and B,[4] it became clear to the authors that a model for accurate evaluation of the energy loss for arbitrary incidence and exit angles cannot be treated by the addition of energy loss along two independent paths. Consequently, in reference,[7] the authors refined the model to evaluate the inelastic scattering cross section of electrons reflected, with any incidence and exit angles in a V-type trajectory, at a specific depth x_0 beneath the surface of a semi-infinite medium, and including the

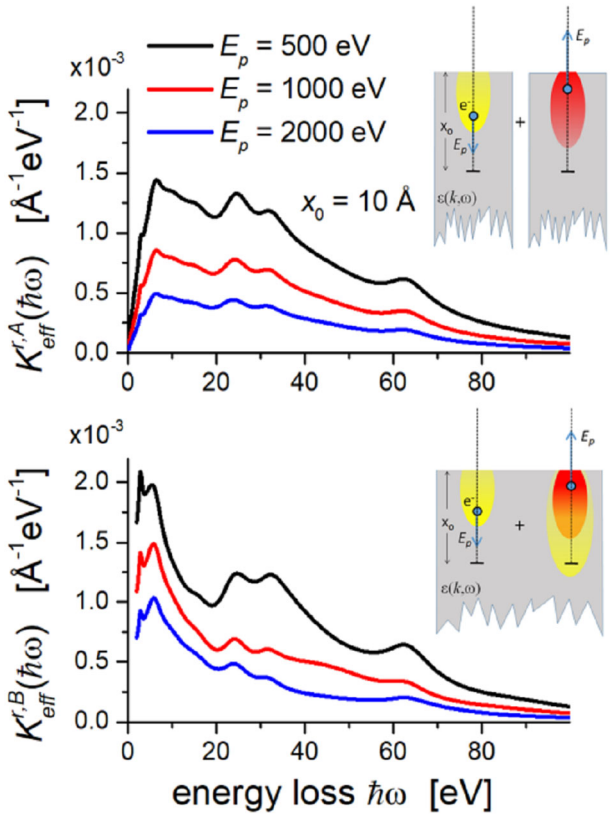

FIGURE 6 Effective inelastic scattering cross sections for electrons with 500, 1000 and 2000 eV energy backscattered in gold at 10 Å depth obtained from Model A (top) and Model B (bottom).[4] The insets show schematic representations of the interaction of the swift electrons where in Model B, the effect on the outgoing electron of the field set up on the way in is included while this is ignored in Model A

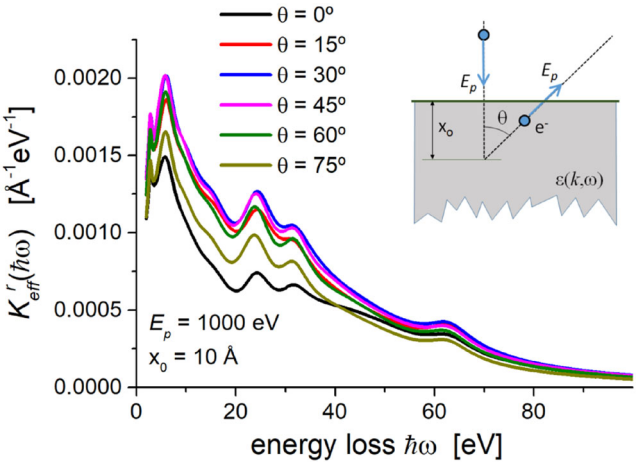

FIGURE 7 Effective inelastic scattering cross sections $K^{r}_{eff}(\hbar\omega)$ for 1000 eV electrons, normal incident on a gold surface and reflected at 10 Å depth into different backscattering angles

effect of the electric field set up around the incoming trajectory on the electron in its outgoing trajectory. Figure 7 shows as an example, the effective inelastic scattering cross sections $K^{r}_{eff}(\hbar\omega)$ for a normal

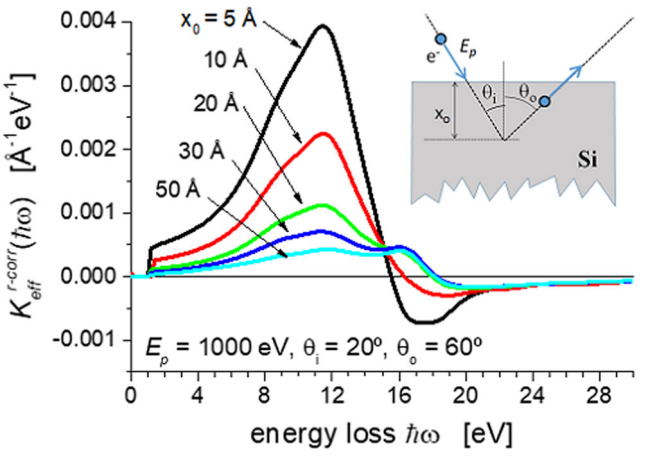

FIGURE 8 Surface correction terms to the effective inelastic scattering cross section $K^{r-corr}_{eff}(\hbar\omega)$ for 1000 eV electrons travelling with a V-type reflection trajectory ($\theta_i = 20°$, $\theta_o = 60°$) on a silicon surface. The effect of varying the backscattering depth between 5 and 50 Å is shown

incident 1000 eV primary electron reflected at depth $x_0 = 10$ Å into various exit angles. Note that the effective cross sections are evaluated as the average energy loss probability per unit path length travelled *inside* the material. Therefore, the effective cross sections in Figure 7 are similar in magnitude although the path length travelled varies considerably. The variation with angle is clear and is caused by the fact that the electric field set up by the incoming electron has not yet died out in the short time before the backscattered electron passes nearby.

A detailed study of this interference effect was performed in reference,[20] where the influence of varying the incidence and exit angles was studied. It was found that the interference effect is non-negligible for all trajectories with an angle between the incoming and outgoing trajectories smaller than 60°.[20]

Note that a V-type trajectory as treated here, where the electron essentially undergoes a single large angle scattering, is the typical case for reflected electrons when the angle of emission is not too large. Thus, Monte Carlo simulations[14] have shown that, in a REELS experiment, about 80% of the total number of electron trajectories can be considered as near V-type, for normal incidence and detection angles up to about 30°.

Similar to Equation 13, the effective cross section can be split up into two terms $K^{r}_{eff}(\hbar\omega) = K(\hbar\omega) + K^{r-corr}_{eff}(\hbar\omega)$ where $K^{r-corr}_{eff}(\hbar\omega)$ is found by subtracting $K(\hbar\omega)$ (Equation 12) from the determined $K^{r}_{eff}(\hbar\omega)$.

The QUEELS software allows to investigate the contribution from individual electrons to the complete energy loss spectra. It is therefore an ideal tool to gain a thorough understanding of the effects that take place at various depths and to compare them quantitatively. For instance, it was used in reference[40] to determine the effective thickness of the surface region, defined as the region in which an electron travelling inside a material will experience surface excitations. In the same paper, QUEELS was used to determine the Begrenzung effect as a function of depth. This is illustrated in Figure 8, which shows the

surface correction contribution K_{eff}^{r-corr} for 1000 eV electrons incident on Si at an angle $\theta_i = 20^\circ$ and coming out at an angle $\theta_o = 60^\circ$ for various backscattering depths. For this case, we have chosen Si as target material because its ELF (taken from reference[41]) is dominated by a sharp plasmon peak. This allows to quantitatively study the increase of the surface plasmon (at ~12 eV) and the negative contribution at the bulk plasmon energy at ~18 eV, which means a reduction in the bulk plasmon intensity (this is the Begrenzung effect) for decreasing backscattering depths.

When the weighted average of K_{eff}^{r} over all depths is considered, as is done in the QUEELS-$\varepsilon(k,\omega)$-REELS software,[17] it was also shown (see, e.g., reference[21]) that the so-called surface excitation parameter (or SEP) can be determined. The SEP is defined as the change in excitation probability for an electron, caused by the presence of the surface, in comparison with an electron travelling in an infinite solid. Moreover, considering results for 27 different materials (including metals, oxides, polymers and semiconductors), a simple equation depending on the generalized plasmon energy and the energy band gap of the material was established.[42] This equation can be applied to estimate the SEP when the dielectric function of the material is not available.

The model in reference[7] allows to discriminate between energy losses in the incoming and outgoing branches of the electron trajectory, as well as those taking place in vacuum and inside the medium. Thus, K_{eff}^{r} can be expressed as a sum of four contributions, which correspond to the energy losses of the electron while travelling in vacuum $K_{eff}^{r,Vi}$ and in the medium $K_{eff}^{r,Mi}$ for the incoming path of the electron trajectory and in vacuum $K_{eff}^{r,Vo}$ and in the medium $K_{eff}^{r,Mo}$ for the outgoing trajectory (see the inset in Figure 9) as

$$K_{eff}^{r}(\hbar\omega) = K_{eff}^{r,Vi}(\hbar\omega) + K_{eff}^{r,Mi}(\hbar\omega) + K_{eff}^{r,Mo}(\hbar\omega) + K_{eff}^{r,Vo}(\hbar\omega) \qquad (14)$$

These four contributions can be plotted and saved separately in QUEELS.

The analytical expressions corresponding to each contribution were reported in reference.[7] Figure 9 shows the corresponding $K_{eff}^{r,Vi}$, $K_{eff}^{r,Mi}$, $K_{eff}^{r,Mo}$ and $K_{eff}^{r,Vo}$ contributions to the effective cross section obtained for electrons of $E_p = 1000$ eV impinging on a gold target with an incident angle $\theta_i = 20^\circ$ and coming out at an angle $\theta_o = 60^\circ$. Note that the separation in Equation 14 into four contributions is not strictly possible because they interfere but it helps to understand the energy loss phenomena occurring along the electron trajectory (as discussed in detail in reference[20]). For example, the cross section can be negative, which reflects the fact that the electron in vacuum on its way to the surface will be attracted by its positive image charge induced in the material. This energy gain corresponds to a negative cross section. This is seen as a negative contribution for $K_{eff}^{r,Vi}$ while the opposite effect occurs in the vacuum part of the outgoing trajectory where the electron is decelerated due to the interaction with its image charge and gives rise to large positive energy losses (as seen in $K_{eff}^{r,Vo}$) at small losses (<20 eV). As expected, surface effects are dominant for small backscattering depths as reported in reference.[7]

It is worth mentioning that evaluation of the inelastic scattering cross section for V-type electron trajectories is the basis for the determination of the dielectric function of surfaces in the ultraviolet (UV) (3–12 eV) and extreme ultraviolet (EUV) (12–120 eV) energy ranges from analysis of REELS experiments. Indeed, by calculating a weighted average of K_{eff}^{r} over relevant path lengths, it is possible to reproduce energy losses occurring in a REELS experiment by adjusting the ELF parameters and in this way determine the ELF of the material. This procedure was implemented in the QUEELS-$\varepsilon(k,\omega)$-REELS software package,[17] and it has been extensively used to determine the ELF and optical properties for many materials.[7,22,23,39,41,43–53]

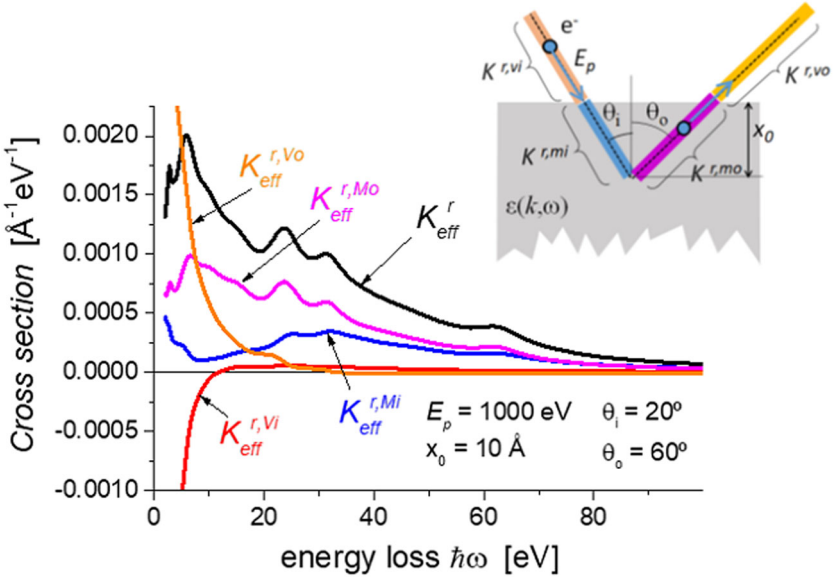

FIGURE 9 $K_{eff}^{r,Vi}$, $K_{eff}^{r,Mi}$, $K_{eff}^{r,Mo}$ and $K_{eff}^{r,Vo}$ (see Equation 14) contributions to the effective inelastic scattering cross section K_{eff}^{r} for an electron travelling in gold within a V-type reflection trajectory ($E_p = 1000$ eV, $\theta_i = 20^\circ$, $\theta_o = 60^\circ$, $x_0 = 10$ Å). The inset illustrates paths that correspond to the individual contributions to K_{eff}^{r}

6 | ELECTRON EMISSION IN PRESENCE OF A STATIC POSITIVE CHARGE (XPS/AES)

In this case, QUEELS evaluates the situation where an electron–hole pair is created at depth x_0 below the surface of a semi-infinite medium as in a typical photoionization process. The model assumes that the photoelectron is created with a certain kinetic energy E_p and leaves the material in a rectilinear trajectory at an emission angle θ with respect to the surface normal, while the positive charge remains at depth x_0 (i.e., with infinite lifetime). Thus, Equation 1 is solved where the external charge $\rho_{ext}(r,t)$ now includes both the moving electron and the static positive charge. The theoretical expressions were derived in reference.[8] The static charge can be varied in the software and choosing +e and +2e corresponds to the XPS and AES situations, respectively. The resulting effective cross section is denoted $K^e_{eff}(\hbar\omega)$.

Figure 10 shows, as an example, $K^e_{eff}(\hbar\omega)$ for 1000 eV electrons emitted in gold at various depths with an emission angle θ of 20° with respect to the surface normal in presence of a positive charge +e.

Figure 11 shows a comparison of cross sections obtained with a static positive charge +e (XPS case) or +2e (AES case) for various depths in Au, with $E_p = 1000$ eV and $\theta = 20°$. Note that the cross sections evaluated in presence of a static +2e charge at the point of electron emission are always larger than those obtained with a + e positive charge. This is because the electric field set up in the medium is larger in the former case and it is present only near this static charge. This corresponds to what is known as the intrinsic energy losses. The difference between AES and XPS electron emission decreases for increasing depth because the relative contribution from intrinsic compared with bulk (known as extrinsic) energy loss decreases for increasing distance travelled by the emitted electron. A review of the energy loss processes in XPS is discussed in reference.[53]

The QUEELS software calculates energy loss processes including both extrinsic and intrinsic excitations for electron emission at a single depth. Often experimental photoelectron and Auger electron emission involves electrons emitted over a range of depths. This can be evaluated by calculating the weighted average of $K^e_{eff}(\hbar\omega)$ over the depths where atoms are present. This procedure was reported in reference[8] and is implemented in the free QUEELS-XPS software package.[18] This software allows to obtain the primary excited spectrum at the point of excitation for XPS (see references[26,27,54–57]) and for AES.[24,25] The calculated spectrum includes excitations caused by the core hole. These spectra were found in references[26,27] to be in good quantitative agreement with first principle quantum mechanical calculations of the detailed excitations in primary excitation spectra for CuO and Fe_2O_3, respectively.

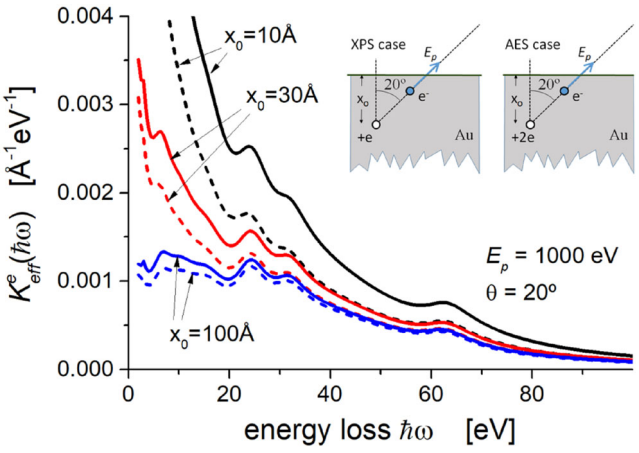

FIGURE 11 Inelastic scattering cross sections $K^e_{eff}(\hbar\omega)$ for 1000 eV electrons emitted at various depths underneath a gold surface with an emission angle $\theta = 20°$ in the presence of a static positive charge +e (X-ray photoelectron spectroscopy [XPS] case, dashed lines) or +2e (Auger electron spectroscopy [AES] case, solid lines)

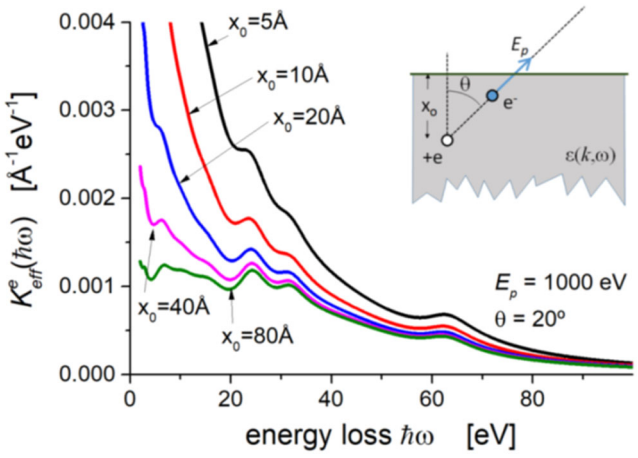

FIGURE 10 Inelastic scattering cross sections $K^e_{eff}(\hbar\omega)$ for 1000 eV electrons emitted at various depths in the presence of a static positive charge +e from a gold surface with an emission angle $\theta = 20°$

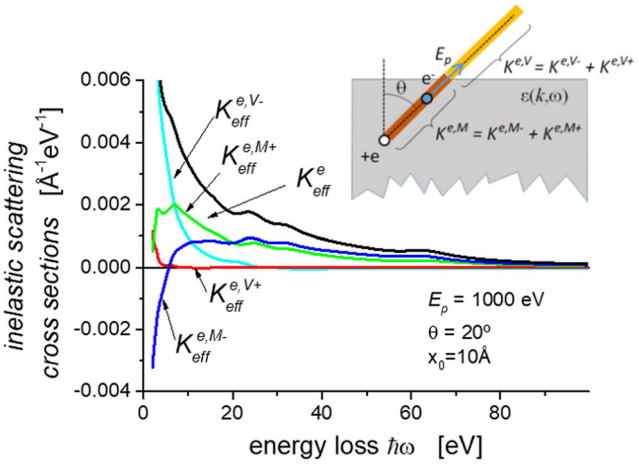

FIGURE 12 Contributions to $K^e_{eff}(\hbar\omega)$ for 1000 eV electrons emitted from a gold surface in presence of a static positive charge +e at a depth $x_0 = 10$ Å with an exit angle $\theta = 20°$. Inset: Schematic representation of the process

In the QUEELS software, it is possible to plot and save the separate contributions from electron energy losses taking place before and after the emitted electron crosses the surface on its way to the detector (extrinsic excitations), and those related to the interaction of the photo/Auger electron with the field set up by the static positive charge (intrinsic excitations). Thus,

$$K^{e}_{eff}(\hbar\omega) = K^{e,V-}_{eff}(\hbar\omega) + K^{e,M-}_{eff}(\hbar\omega) + K^{e,M+}_{eff}(\hbar\omega) + K^{e,V+}_{eff}(\hbar\omega) \qquad (15)$$

where the subscripts V and M refer to energy losses, occurring when the electron moves in vacuum or in the medium, respectively, and the subscripts $-$ and $+$ refer to losses due to the interaction of the swift electron with the field set up by the moving electron itself and by the static positive charge, respectively.

Figure 12 shows, as an example, the different contributions to the effective inelastic scattering cross section K^{e}_{eff} for emission of 1000 eV electrons in gold 10 Å beneath the surface with an emission angle of 20°. It is instructive to explore the individual contributions to the total energy loss. This can be used to quantitatively evaluate the partition between extrinsic and intrinsic excitations within the photoelectron emission process.[58]

As mentioned above, the energy losses in experimental photoelectron or Auger electron emission can be evaluated by calculating the weighted average of K^{e}_{eff} over the depths where the corresponding atoms are present. This procedure was reported in reference[8] and is implemented in the free QUEELS-XPS software package.[18]

7 | SHORT USER'S GUIDE

Sections 3–6 outlined the theoretical dielectric response framework that is implemented in QUEELS and allows to evaluate inelastic scattering cross sections of swift electrons interacting with matter in several configurations. Although the use of QUEELS software is rather intuitive, an extensive guide is included in the supporting information. In this section, we present a short description to illustrate the structure and ease of use to possible interested users.

The main QUEELS dialog window is shown in Figure 13. The first step for the calculations is to set up the dielectric properties of the studied material. This is done by selecting the 'Set Material Parameters' button, which opens a new window as seen in Figure 14A. Here, the user should input parameters for each oscillator corresponding to Equations 9 and 10, which defines the ELF function. This set can be saved to a file (with the Save button), which can later be read. Files with the set of oscillators for several materials are available.[33] Saved ELFs can be loaded by first locating the folder and file with the file manager (see Figure 15) and then clicking the Read button.

After specifying the dielectric function, the other buttons 'Electron travelling in a homogeneous isotropic medium', 'Electron passing through a thin film', 'Electron reflected from a surface. Normal incidence and exit angles', 'Electron reflected from a surface. Any incidence and exit angle' and 'Photon and Auger excited electrons' will allow to perform the calculation of effective cross sections corresponding to the situations in Sections 3, 4, 5.1, 5.2 and 6, respectively. When they are selected, a new dialog window opens as shown in Figure 14B–F, respectively.

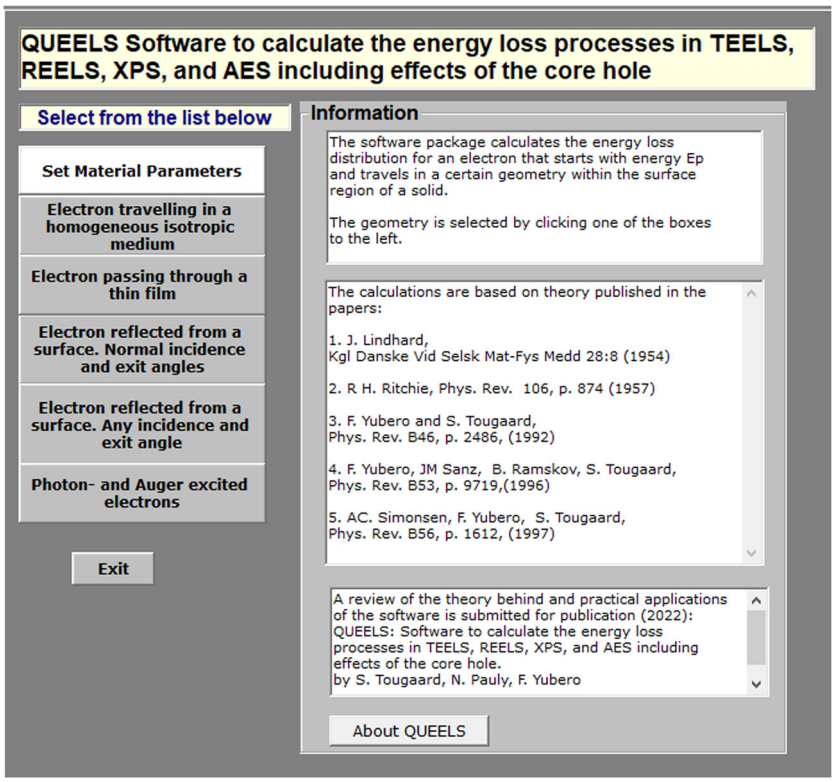

FIGURE 13 Initial QUEELS dialog screen

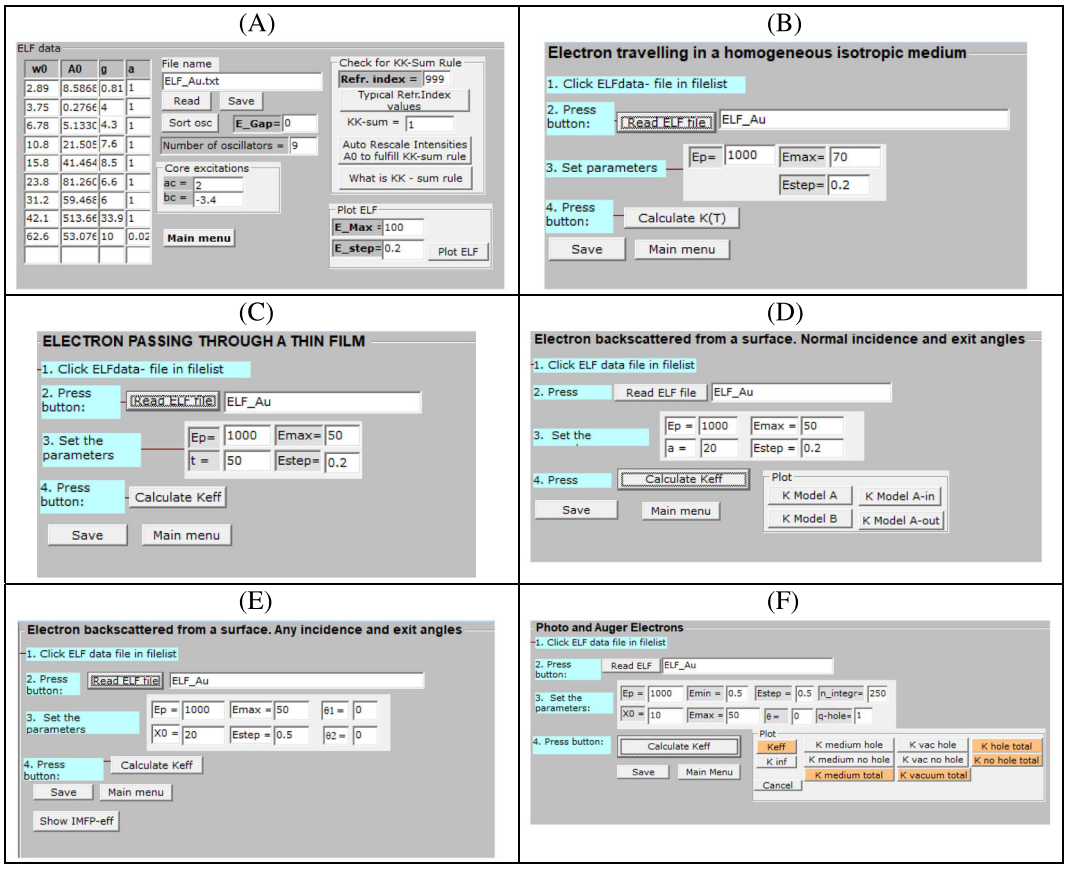

FIGURE 14 Parameter-dialog windows in QUEELS for the evaluation of electron inelastic scattering cross sections: (A) ELF oscillator parameters, (B) homogeneous isotropic medium, (C) transmission through a thin foil, (D) reflection: normal incidence and exit angles, (E) reflection: any incidence and exit angles and (F) emission in the presence of a positive charge

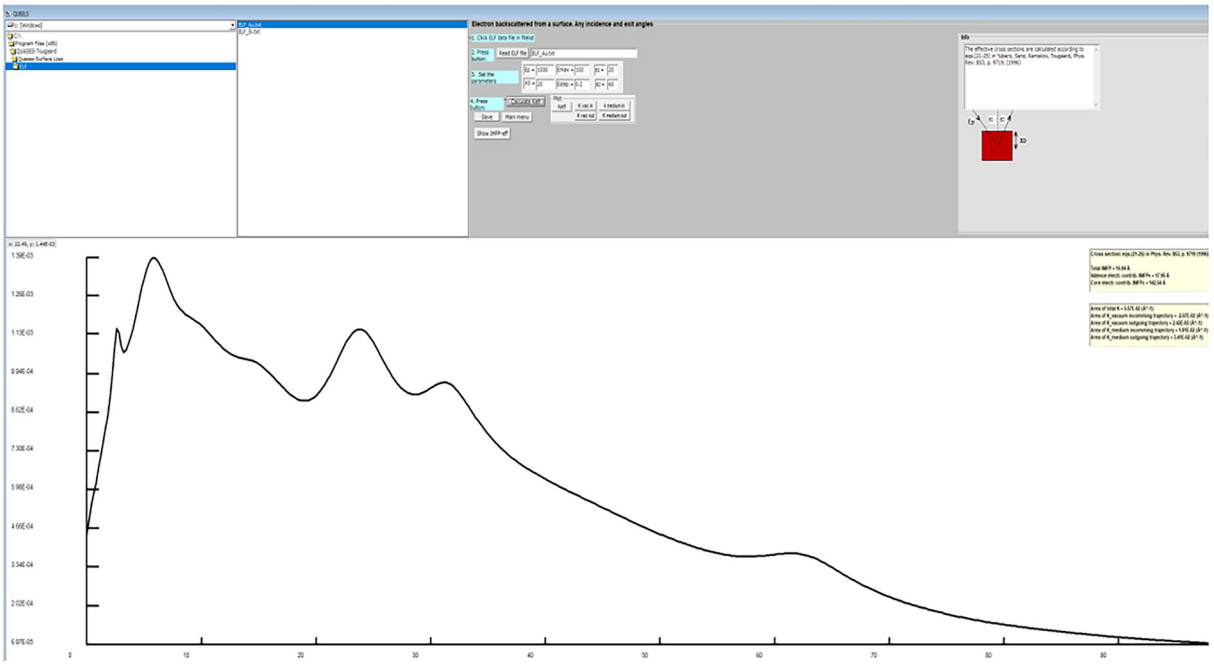

FIGURE 15 The screen with dialog windows that appear after selecting one of the structures in the main menu (Figure 12). Here exemplified by the choice 'Backscattering from a surface. Any incidence and exit angle'. The calculated effective cross section is for a 1000 eV electron impinging on gold at 20° incidence and 60° exit angles after being backscattered at 20 Å depth

The structure of the dialog window is similar for all cases, and in Figure 15, it is exemplified by the case 'Backscattering from a surface. Any incidence and exit angle'. The screen is composed of a *File-manager window* (the upper left part), a *Parameter-dialog window* (the upper middle part), a window that shows the structure being evaluated (the upper right part) and a *Graph window* (the lower part) (see Figure 15). The *File-manager window*, in the upper left corner of the dialog screens, allows to navigate through the folder structure of the computer where the software is installed. This is applied to select the folder where the files with the set of oscillators for the material are stored. It is also used to determine where the calculated cross sections are saved. In the *Parameter-dialog window* located in the upper central part of the screens, the parameters for the calculation are set. The first step is to read the data file that describes the dielectric function of the considered material. This is done by first find and select the file with the appropriate ELF oscillators in the File manager (in this case Au-ELF valid for gold) and then clicking the 'Read ELF file' button. The next step is to specify the geometry of the considered situation (in this case they are the depth x_0 in Å, the incidence and exit angles, the electron energy E_p in eV, the maximum energy loss considered [E_{max}] and the energy grid in the calculations [E_{step}]). Finally, by clicking the button 'Calculate Keff', the inelastic scattering cross section is evaluated and plotted in the *Graph window*. The calculated cross section can be saved to a file by clicking the Save button. The insets in the upper right corner of the graph window (yellow boxes) display the corresponding effective inelastic mean free path, evaluated according to Equations 6–8.

The *Parameter-dialog window* is slightly different for the cases as shown in Figure 14 and the meaning of the input parameters is rather intuitive corresponding to each case. The units are in all cases Å and eV.

To get acquainted with the QUEELS software, it can be instructive and useful for the user to go through the examples shown in the figures in this paper. This is easily done by using the set of ELF functions for Si and Au provided in the supporting information.

8 | SUMMARY

The QUEELS software package is presented. Within a dielectric response model, it evaluates inelastic scattering cross sections for electrons travelling nearby surfaces in several environments (homogeneous isotropic medium, through thin foil, V-type reflection trajectory at a surface and emission in the presence of a positive charge). We present the theoretical basis as well as specific applications for each situation. The dielectric function in the form of the ELF is the only input in the software, and we have compiled a database of ELF parameters for various materials, taken from previous publications that can be downloaded from reference.[33] Finally, we join an extended user's manual in the supporting information.

ORCID

Sven Tougaard https://orcid.org/0000-0003-0909-8764
Nicolas Pauly https://orcid.org/0000-0002-0368-6939
Francisco Yubero https://orcid.org/0000-0001-5107-9490

REFERENCES

1. Gauglitz G, Vo-Dinh T. *Handbook of Spectroscopy*. Weinheim: WileyVCH; 2003; 538p. doi:10.1002/3527602305
2. Lindhard J. On the properties of a gas of charged particles. *K Dan Vidensk Selsk Mat Fys Medd*. 1954;28:1-57.
3. Ritchie RH. Plasma losses by fast electrons in thin films. *Phys Rev*. 1957;106(5):874-881. doi:10.1103/PhysRev.106.874
4. Yubero F, Tougaard S. Model for quantitative analysis of reflection-electron energy-loss spectra. *Phys Rev B*. 1992;46(4):2486-2497. doi:10.1103/PhysRevB.46.2486
5. Ritchie RH, Marusak AL. The surface plasmon dispersion relation for an electron gas. *Surf Sci*. 1966;4(3):234-240. doi:10.1016/0039-6028(66)90003-3
6. Gervasoni JL, Arista NR. Energy loss and plasmon excitation during electron emission in the proximity of a solid surface. *Surf Sci*. 1992;260(1-3):329-346. doi:10.1016/0039-6028(92)90049-C
7. Yubero F, Sanz JM, Ramskov B, Tougaard S. Model for quantitative analysis of reflection-electron-energy-loss spectra: angular dependence. *Phys Rev B*. 1996;53(15):9719-9727. doi:10.1103/PhysRevB.53.9719
8. Simonsen AC, Yubero F, Tougaard S. Quantitative model of electron energy loss in XPS. *Phys Rev B*. 1997;56(3):1612-1619. doi:10.1103/PhysRevB.56.1612
9. Novak M, Egri S, Kover L, Cserny I, Drube W, Werner WSM. Energy dependence of electron energy loss processes in Ge 2s photoemission. *Surf Sci*. 2007;601(11):2344-2351. doi:10.1016/j.susc.2007.03.039
10. Tung CJ, Chen YF, Kwei CM, Chou TL. Differential cross sections for plasmon excitations and reflected electron-energy-loss spectra. *Phys Rev B*. 1994;49(23):16684-16693. doi:10.1103/PhysRevB.49.16684
11. Yubero F, Tougaard S. Quantitative analysis of reflection electron energy-loss spectra. *Surf Interface Anal*. 1992;19(1-12):269-273. doi:10.1002/sia.740190152
12. Li YC, Tu YH, Kwei CM, Tung CJ. Influence of the direction of motion on the inelastic interaction between electrons and solid surfaces. *Surf Sci*. 2005;589:67-76
13. Ding ZJ. Self-energy in surface electron spectroscopy: I. Plasmons on a free-electron-material surface. *J Phys Condens Matter*. 1998;10(8):1733-1751. doi:10.1088/0953-8984/10/8/009
14. Yubero F, Pauly N, Dubus A, Tougaard S. Test of validity of the V-type approach for electron trajectories in reflection electron energy loss spectroscopy. *Phys Rev B*. 2008;77(24):1-11, 245405 doi:10.1103/PhysRevB.77.245405
15. Tougaard S, Yubero F. QUEELS software for calculation of energy loss processes in TEELS, REELS, XPS, and AES including effects of the core hole (2.3). Zenodo. 2022. https://doi.org/10.5281/zenodo.6022426
16. Tougaard S, Yubero F. QUEELS software package for calculation of surface effects in electron spectra. *Surf Interface Anal*. 2004;36(8):824-827. doi:10.1002/sia.1774
17. Tougaard S, Yubero F. QUEELS-$\varepsilon(k,\omega)$-REELS: software package for quantitative analysis of electron energy loss spectra; dielectric function determined by reflection electron energy loss spectroscopy. Version 1.1. 2006. http://www.quases.com
18. Tougaard S, Yubero F. QUEELS-XPS software package: quantitative analysis of electron energy loss in XPS spectra. Ver. 2.1. 2011. http://quases.com/products/queels-xps/ also available at https://doi.org/10.5281/zenodo.6413959
19. Pauly N, Tougaard S, Yubero F. Theoretical study of the surface excitation parameter from reflection-electron-energy-loss spectra. *Surf Interface Anal*. 2005;37(13):1151-1157. doi:10.1002/sia.2126
20. Pauly N, Yubero F, Tougaard S. Oscillating surface effect in reflection-electron energy-loss spectra. *Phys Rev B*. 2006;73(3):1-11, 035402. doi:10.1103/PhysRevB.73.035402
21. Pauly N, Tougaard S. Theoretical determination of the surface excitation parameter for Ti, Fe, Cu, Pd, Ag, and Au. *Surf Sci*. 2007;601(23):5611-5615. doi:10.1016/j.susc.2007.09.034

22. Yubero F, Fujita D, Ramskov B, Tougaard S. Experimental test of model for angular and energy dependence of reflection electron energy loss spectra. *Phys RevB*. 1996;53(15):9728-9732. doi:10.1103/PhysRevB.53.9728
23. Hajati S, Romanyuk O, Zemek J, Tougaard S. Validity of Yubero-Tougaard theory to quantitatively determine the dielectric properties of surface nanofilms. *Phys Rev B*. 2008;77(15):1-11, 155403 doi:10.1103/PhysRevB.77.155403
24. Berényi Z, Kövér L, Tougaard S, et al. Contribution of intrinsic and extrinsic excitations to KLL Auger spectra induced from Ge films. *J Electron Spectrosc Relat Phenom*. 2004;135(2-3):177-182. doi:10.1016/j.elspec.2004.03.005
25. Pauly N, Tougaard S, Yubero F. LMM Auger primary excitation spectra of copper. *Surf Sci*. 2014;630:294-299. doi:10.1016/j.susc.2014.08.029
26. Pauly N, Tougaard S, Yubero F. Determination of the Cu 2p primary excitation spectra for Cu, Cu_2O and CuO. *Surf Sci*. 2014;620:17-22. doi:10.1016/j.susc.2013.10.009
27. Pauly N, Yubero F, Espinós JP, Tougaard S. XPS primary excitation spectra of Zn 2*p*, Fe 2*p*, and Ce 3*d* from ZnO, α-Fe_2O_3, and CeO_2. *Surf Interface Anal*. 2019;51:353-360. doi:10.1002/sia.6587
28. Tanuma S, Powell CJ, Penn DR. Calculations of electron inelastic mean free paths. V. Data for 14 organic compounds over the 50–2000 eV range. *Surf Interface Anal*. 1994;21(3):165-176. doi:10.1002/sia.740210302
29. Powell CJ. Attenuation lengths of low-energy electrons in solids. *Surf Sci*. 1974;44(1):29-46. doi:10.1016/0039-6028(74)90091-0
30. Penn DR. Quantitative chemical analysis by ESCA. *J Electron Spectrosc Relat Phenom*. 1976;9(1):29-40. doi:10.1016/0368-2048(76)85004-9
31. Ritchie RH, Howie A. Electron excitation and the optical potential in electron microscopy. *Philos Mag*. 1977;36(2):463-481. doi:10.1080/14786437708244948
32. Pines D, Nozieres P. *The Theory of Quantum Liquids*. Boca Raton: CRC Press; 1999:576.
33. Pauly N, Yubero F, Tougaard S. ELF dielectric functions for various materials. (1.0) [Data set]. Zenodo. 2022. https://doi.org/10.5281/zenodo.6024064
34. Pauly N, Tougaard S. Model for Monte Carlo simulations of reflection electron energy loss spectra applied to silicon at energies between 300 and 2000 eV. *Surf Interface Anal*. 2010;42(6-7):1100-1104. doi:10.1002/sia.3277
35. Tougaard S. QUASES: software packages to characterize surface nano-structures by analysis of electron spectra. Version 7.5. 2021. http://www.quases.com/
36. Tougaard S. Universality classes of inelastic electron scattering cross-sections. *Surf Interface Anal*. 1997;25(3):137-154. doi:10.1002/(SICI)1096-9918(199703)25:3%3C137::AID-SIA230%3E3.0.CO;2-L
37. Ewels P, Sikora T, Serin V, Ewels CP, Lajaunie L. A complete overhaul of the electron energy-loss spectroscopy and X-ray absorption spectroscopy database: eelsdb.eu. *Microsc Microanal*. 2016;22(3):717-724. doi:10.1017/S1431927616000179
38. Tougaard S. QUASES-Inelastic electron mean free path calculator (by TPP2M formula) (4.2). Zenodo. 2021. https://doi.org/10.5281/zenodo.5707501
39. Pauly N, Yubero F, Espinos JP, Tougaard S. Optical properties and electronic transitions of zinc oxide, ferric oxide, cerium oxide, and samarium oxide in the ultraviolet and extreme ultraviolet. *Appl Optics*. 2017;56(23):6611-6621. doi:10.1364/AO.56.006611
40. Pauly N, Tougaard S. Determination of the effective surface region thickness and of Begrenzung effect. *Surf Sci*. 2009;603(13):2158-2162. doi:10.1016/j.susc.2009.04.023
41. Yubero F, Tougaard S, Elizalde E, Sanz JM. Dielectric loss function of Si and SiO_2 from quantitative analysis of REELZS spectra. *Surf Interface Anal*. 1993;20(8):719-726. doi:10.1002/sia.740200817
42. Pauly N, Tougaard S. Surface excitation parameter for 12 semiconductors and determination of a general predictive formula. *Surf Interface Anal*. 2009;41(9):735-740. doi:10.1002/sia.3081
43. Yubero F, Sanz JM, Trigo JF, Elizalde E, Tougaard S. Quantitative analysis of REELS spectra of ZrO_2: determination of the dielectric loss function and inelastic mean free paths. *Surf Interface Anal*. 1994;22(1-12):124-128. doi:10.1002/sia.740220130
44. Jin H, Oh SK, Kang HJ, Tougaard S. Electronic properties of ultrathin HfO_2, Al_2O_3, and Hf–Al–O dielectric films on Si(100) studied by quantitative analysis of reflection electron energy loss spectra. *J Appl Phys*. 2006;100(8):083713. doi:10.1063/1.2360382
45. Tahir D, Lee EK., Oh SK., et al. Dielectric and optical properties of Zr silicate thin films grown on Si(100) by atomic layer deposition, *J Appl Phys*. 2019; 106(8):084108. doi:10.1063/1.3246612
46. Denny Y, Shin H, Seo S, et al. Electronic and optical properties of hafnium indium zinc oxide thin film by XPS and REELS. *J Electron Spectrosc Relat Phenom*. 2012;185(1-2):18-22. doi:10.1016/j.elspec.2011.12.004
47. Tahir D, Tougaard S. Electronic and optical properties of selected polymers studied by reflection electron spectroscopy, *J Appl Phys*. 2012;111(5):054101. doi:10.1063/1.3688327
48. Tahir D, Tougaard S. Electronic and optical properties of Cu, CuO and Cu_2O studied by electron spectroscopy, *J Phys Condens Matter*. 2012;24(17):175002. doi:10.1088/0953-8984/24/17/175002
49. Tahir D, Kraaer J, Tougaard S. Electronic and optical properties of Fe, Pd, and Ti studied by reflection electron energy loss spectroscopy. *J Appl Phys*. 2014;115(24):243508. doi:10.1063/1.4885876
50. Tahir D, Oh SK, Kang HJ, Tougaard S. Quantitative analysis of reflection electron energy loss spectra to determine electronic and optical properties of Fe–Ni alloy thin films. *J Electron Spectrosc Related Phenom*. 2016;206:6-11. doi:10.1016/j.elspec.2015.11.005
51. Tahir D, Oh SK, Kang HJ, Tougaard S. Composition dependence of dielectric and optical properties of Hf-Zr-silicate thin films grown on Si(100) by atomic layer deposition. *Thin Solid Films*. 2016;616:425-430. doi:10.1016/j.tsf.2016.09.001
52. Pauly N, Yubero F, Tougaard S. Optical properties of molybdenum in the ultraviolet and extreme ultraviolet by reflection electron energy loss spectroscopy. *Appl Optics*. 2020;59(14):4527-4532. doi:10.1364/AO.391014
53. Tougaard S. Energy loss in XPS: Fundamental processes and applications for quantification, non-destructive depth profiling and 3D imaging. *J Electron Spectrosc Related Phenom*. 2010;178:128-153. doi:10.1016/j.elspec.2009.08.005
54. Pauly N, Yubero F, Tougaard S. Quantitative analysis of Yb 4d photoelectron spectrum of metallic Yb. *Surf Interface Anal*. 2018;50(11):1168-1173. doi:10.1002/sia.6402
55. Pauly N, Yubero F, Tougaard S. Quantitative analysis of satellite structures in XPS spectra of gold and silver. *Appl Surf Sci*. 2016;383:317-323. doi:10.1016/j.apsusc.2016.03.185
56. Pauly N, Yubero F, Garcia-Gariıa F-J, Tougaard S. Quantitative analysis of Ni 2p photoemission in NiO and Ni diluted in a SiO_2 matrix. *Surf Sci*. 2016;644:46-52. doi:10.1016/j.susc.2015.09.012
57. Yubero F, Kover L, Drube W, Eickhoff T, Tougaard S. Test of dielectric–response model for energy and angular dependence of plasmon excitations in core-level photoemission. *Surf Sci*. 2005;592(1–3):1-7. doi:10.1016/j.susc.2005.06.028
58. Gnacadja E, Pauly N, Tougaard S. Universal inelastic electron scattering cross section including extrinsic and intrinsic excitations in XPS. *Surf Interface Anal*. 2020;52(7):413-421. doi:10.1002/sia.6749
59. Emfietzoglou D, Cucinotta FA, Nikjoo H. A complete dielectric response model for liquid water: a solution of the Bethe Ridge problem. *Radiat Res*. 2005;164(2):202-211. doi:10.1667/RR3399

60. Egerton RF. *Electron Energy-Loss Spectroscopy in the Electron Microscope*, 2nd ed. New York: Plenum Press; 1996; 485 pp. 10.1007/978-1-4757-5099-7

SUPPORTING INFORMATION

Additional supporting information may be found in the online version of the article at the publisher's website.

How to cite this article: Tougaard S, Pauly N, Yubero F. QUEELS: Software to calculate the energy loss processes in TEELS, REELS, XPS and AES including effects of the core hole. *Surf Interface Anal*. 2022;1-14. doi:10.1002/sia.7095